Matrix based Subdivision Depth Computation for Extra-Ordinary Catmull-Clark Subdivision Surface Patches

Gang Chen and Fuhua (Frank) Cheng
Graphics and Geometric Modeling Lab, Department of Computer Science
University of Kentucky, Lexington, Kentucky 40506-0046

Abstract

A new subdivision depth computation technique for extra-ordinary Catmull-Clark subdivision surface (CCSS) patches is presented. The new technique improves a previous technique by using a matrix representation of the second order norm in the computation process. This enables us to get a more precise estimate of the rate of convergence of the second order norm of an extra-ordinary CCSS patch and, consequently, a more precise subdivision depth for a given error tolerance.

Keywords: subdivision surfaces, subdivision depth computation

1 Introduction

Given a Catmull-Clark subdivision surface (CCSS) patch, *subdivision depth computation* is the process of determining how many times the control mesh of the CCSS patch should be subdivided so that the distance between the resulting control mesh and the surface patch is smaller than a given error tolerance. Good subdivision depth computation techniques are important because they allows us to meet precision requirement in applications such as *trimming*, *finite element mesh generation*, *boolean operations*, and *tessellation* of a CCSS without excessively subdividing its control mesh.

A good subdivision depth computation technique requires precise estimate of the distance between the control mesh of a CCSS patch and its limit surface. Optimum distance evaluation techniques for regular CCSS patches are available [4, 11]. Distance evaluation for an extra-ordinary CCSS patch is more complicated. A first attempt in that direction is done in [4]. The distance is evaluated by measuring norms of the *first order forward differences* of the control points. Since first order forward differences can not measure the curvature of a surface but its dimension, the distance computed by this approach is usually bigger than what it really is for regions already flat enough and, consequently, leads to over-estimated subdivision depth.

An improved distance evaluation technique for extra-ordinary CCSS patches is presented in [5]. The distance is evaluated by measuring norms of the *second order forward differences* (called *second order norms*) of the control points of the given extra-ordinary CCSS patch. Since second order forward differences can measure both height and width of a region, the distance computed by this approach reflects curvature of the patch and, hence, leads to reasonable subdivision depths for regions already flat enough. However, it has been observed recently that, for extra-ordinary CCSS patches, the convergence rate of second order norm changes with the subdivision process, especially between the first subdivision level and the second subdivision level. Therefore, using a fixed convergence rate in the distance evaluation process for all subdivision levels would over-estimate the distance and, consequently, over-estimate the subdivision depth as well.

In this paper we present an improved subdivision depth computation method for extra-ordinary CCSS patches. The new technique uses a matrix representation of the maximum second order norm in the computation process to generate a recurrence formula. This recurrence formula allows the smaller convergence rate of the second subdivision level to be used as a bound in the evaluation of the maximum second order norm and, consequently, leads to a more precise subdivision depth for the given error tolerance.

The remaining part of the paper is arranged as follows. A brief review of the background is given in Section 2. A matrix based subdivision depth computation technique for extra-ordinary CCSS patches is presented in section 3. Examples showing the new technique improves the old one are presented in Section 4. Concluding remarks are given in Section 5.

2 Problem Formulation and Background

Given the control mesh of an extra-ordinary CCSS patch and an error tolerance ϵ, the goal here is to compute an integer d so that if the control mesh is iteratively refined (subdivided) d times, then the distance between the resulting mesh and the surface patch is smaller than ϵ. d is called the *subdivision depth* of the surface patch with

respect to ϵ. Before we show the new computation technique, we need to define related terms and review the previous, second order norm based distance evaluation and subdivision depth computation techniques for extra-ordinary CCSS patches [5]. Some of these techniques are needed in the new technique to be presented in Section 3.

2.1 Catmull-Clark Subdivision Surfaces

Given a control mesh, by iteratively applying the *Catmull-Clark subdivision scheme* [2] to refine (subdivide) the control mesh, we get a sequence of refined control meshes. The *limit surface* of the refined control meshes is called a *Catmull-Clark subdivision surface* (CCSS). The refining process consists of defining new vertices (*face points*, *edge points* and *vertex points*) and connecting the new vertices to form new edges and faces of a new control mesh. The control mesh of a CCSS patch and the new control mesh after a refining (subdivision) process are shown in Figures 1(a) and 1(b), respectively. This is a conceptual drawing, the location shown for a new vertex might not be its exact physical location.

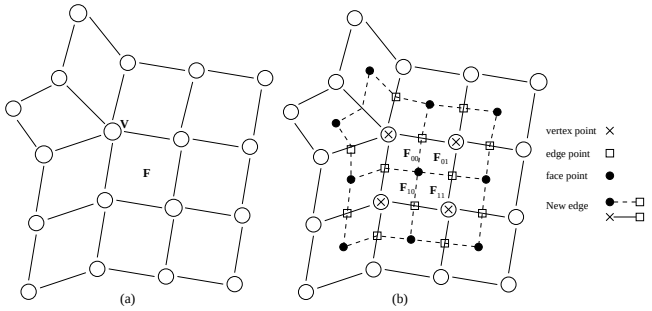

Figure 1: (a) Control mesh of an extra-ordinary patch; (b) new vertices and edges generated after a Catmull-Clark subdivision.

The limit surface of the iteratively refined control meshes is called a *subdivision surface* because the mesh refining process is a generalization of the uniform bicubic B-spline surface subdivision technique. Therefore, CCSSs include uniform B-spline surfaces and piecewise Bézier surfaces as special cases. Actually CCSSs include non-uniform B-spline surfaces and NURBS surfaces as special cases as well [13]. The Catmull-Clark mesh refining process sometime will also be called a *Catmull-Clark subdivision*, or simply a *subdivision step*. The given control mesh will be referred to as $\mathbf{M}_0$ and the limit surface will be referred to as $\bar{\mathbf{S}}$. For each positive integer k, $\mathbf{M}_k$ refers to the control mesh obtained after applying the Catmull-Clark subdivision k times to $\mathbf{M}_0$.

2.2 Regular vs. Extra-ordinary

The power of CCSSs comes from the way mesh vertices are connected. If the number of edges incident to a mesh vertex is called its *valence*, then the valence of an interior mesh vertex can be anything ≥ 3, instead of just four. Those mesh vertices whose valences are different from four are called *extra-ordinary vertices* to distinguish them from the *standard* or *regular mesh vertices*. Vertex $\mathbf{V}$ in Figure 1(a) is an extra-ordinary vertex of valence five. An interior mesh face is called an *extra-ordinary mesh face* if it has an extra-ordinary vertex. Otherwise, a *standard* or *regular mesh face*. Mesh face $\mathbf{F}$ in Figure 1(a) is an extra-ordinary mesh face. Note that after one iteration of the subdivision step, mesh faces of a CCSS are always quadrilaterals and the number of extra-ordinary vertices remains the same. After at most two iterations of the subdivision step, each mesh face has at most one extra-ordinary vertex. Therefore, without loss of generality, we shall assume all the mesh faces in $\mathbf{M}_0$ are quadrilaterals and each mesh face of $\mathbf{M}_0$ has at most one extra-ordinary vertex.

For each interior face $\mathbf{F}$ of $\mathbf{M}_k$, $k \geq 0$, there is a corresponding patch $\mathbf{S}$ in the limit surface $\bar{\mathbf{S}}$. $\mathbf{F}$ and $\mathbf{S}$ can be parametrized on the same parameter space $\Omega = [0,\ 1] \times [0,\ 1]$ [14]. $\mathbf{F}$ is a bilinear *rule surface*. $\mathbf{S}$ is a uniform bicubic B-spline surface patch if $\mathbf{F}$ is a regular face. If $\mathbf{F}$ is an extra-ordinary face then $\mathbf{S}$, defined by $2n + 8$ control points where n is the valence of $\mathbf{F}$'s extra-ordinary vertex, can not be parametrized as a uniform B-spline patch. In such a case, $\mathbf{S}$ is called an *extra-ordinary surface patch*. Otherwise, a *regular surface patch* or *standard surface patch*. The control mesh shown in Figure 1(a) is the control mesh of an extra-ordinary surface patch whose extra-ordinary vertex is of valence five.

2.3 Distance and Subdivision Depth

For a given interior mesh face $\mathbf{F}$, let $\mathbf{S}$ be the corresponding patch in the limit surface $\bar{\mathbf{S}}$. The control mesh of $\mathbf{S}$ contains $\mathbf{F}$ as the center face. If we perform a subdivision step on the control mesh, we get four new mesh faces in the place of $\mathbf{F}$. This is the case no matter $\mathbf{F}$ is a regular face or an extra-ordinary face. See Figure 1(b) for the four new faces $\mathbf{F}_{00}$, $\mathbf{F}_{10}$, $\mathbf{F}_{01}$ and $\mathbf{F}_{11}$ in the place of the extra-ordinary face $\mathbf{F}$ shown in Figure 1(a). Since each of these new faces corresponds to a quarter subpatch of $\mathbf{S}$, we shall call these new faces *subfaces* of $\mathbf{F}$ even though they are not pyhsically subsets of $\mathbf{F}$. Therefore, each subdivision step generates four new subfaces for the center face $\mathbf{F}$ of the control mesh. Because the correspondence between $\mathbf{F}$ and $\mathbf{S}$ is one-to-one, sometime, instead of saying performing a subdivision step on $\mathbf{S}$, we simply say performing a subdivision step on $\mathbf{F}$.

The *distance* between an interior mesh face $\mathbf{F}$ and the corresponding patch $\mathbf{S}$ is defined as the maximum of $\|\mathbf{F}(u,v) - \mathbf{S}(u,v)\|$:

$$D_{\mathbf{F}} = max_{(u,v)\in\Omega} \|\mathbf{F}(u,v) - \mathbf{S}(u,v)\| \qquad (1)$$

where Ω is the unit square parameter space of $\mathbf{F}$ and $\mathbf{S}$. $D_{\mathbf{F}}$ is also called the distance between $\mathbf{S}$ and its control mesh. For a given $\epsilon > 0$, the *subdivision depth* of $\mathbf{F}$ with respect to ϵ is a positive integer d such that if $\mathbf{F}$ is recursively subdivided d times, the distance between each of the resulting subfaces and the corresponding subpatch is smaller than ϵ.

2.4 Distance Evaluation for a Regular Patch

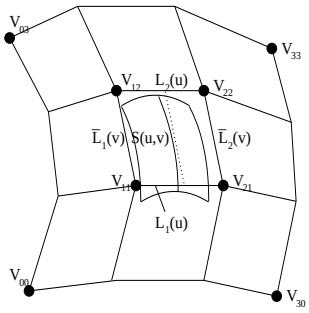

Figure 2: Definition of $\mathbf{L}(u,v) = (1-v)\mathbf{L}_1(u) + v\mathbf{L}_2(u) = (1-u)\bar{\mathbf{L}}_1(v) + u\bar{\mathbf{L}}_2(v)$.

Let $\mathbf{S}(u,v)$ be a uniform bicubic B-spline surface patch defined on the unit square $\Omega = [0,1] \times [0,1]$ with control points $\mathbf{V}_{i,j}$, $0 \le i,j \le 3$, and let $\mathbf{L}(u,v)$ be the bilinear parametrization of the center mesh face $\{\mathbf{V}_{1,1}, \mathbf{V}_{2,1}, \mathbf{V}_{2,2}, \mathbf{V}_{1,2}\}$ (see Figure 2):

$$\begin{aligned}\mathbf{L}(u,v) &= (1-v)[(1-u)\mathbf{V}_{1,1} + u\mathbf{V}_{2,1}] \\ &\quad +v[(1-u)\mathbf{V}_{1,2} + u\mathbf{V}_{2,2}], \quad 0 \le u,v \le 1.\end{aligned}$$

The distance between $\mathbf{S}(u,v)$ and $\mathbf{L}(u,v)$ satisfies the following relationship [4].

Lemma 1: The distance between $\mathbf{L}(u,v)$ and $\mathbf{S}(u,v)$ satisfies the following inequality

$$\max_{0 \le u,v \le 1} \|\mathbf{L}(u,v) - \mathbf{S}(u,v)\| \le \frac{1}{3}M$$

where M is the *second order norm* of $\mathbf{S}(u,v)$ defined as follows

$$\begin{aligned}M &= \max_{i,j}\{\, \|2\mathbf{V}_{i,j} - \mathbf{V}_{i-1,j} - \mathbf{V}_{i+1,j}\|\,, \\ &\qquad \|2\mathbf{V}_{i,j} - \mathbf{V}_{i,j-1} - \mathbf{V}_{i,j+1}\| \,\}\end{aligned} \tag{2}$$

2.5 Subdivision Depth Computation for Extra-Ordinary Patches

The distance evaluation mechanism of the previous subdivision depth computation technique for extra-ordinary CCSS patches utilizes second order norm as a measurement scheme as well [5], but the pattern of second order forward differences (SOFDs) used in the distance evaluation process is different from (2). We review the definition of SOFD pattern used for an extra-ordinary patch and a recurrence formula for the corresponding second order norm first.

2.5.1 Second Order Norm and Recurrence Formula

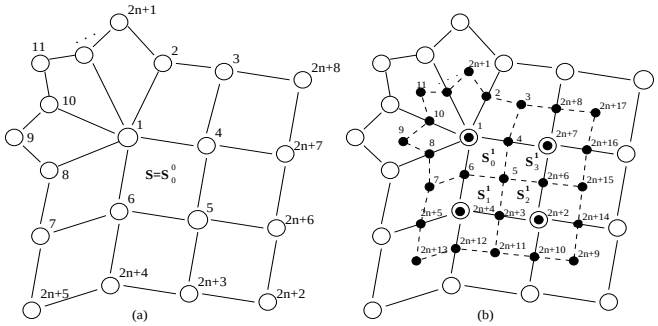

Figure 3: (a) Ordering of control points of an extra-ordinary patch. (b) Ordering of new control points (solid dots) after a Catmull-Clark subdivision.

Let $\mathbf{V}_i$, $i = 1, 2, ..., 2n+8$, be the control points of an extra-ordinary patch $\mathbf{S}(u,v) = \mathbf{S}_0^0(u,v)$, with $\mathbf{V}_1$ being an extra-ordinary vertex of valence n. The control points are ordered following J. Stam's fashion [14] (Figure 3(a)). The control mesh of $\mathbf{S}(u,v)$ is denoted $\Pi = \Pi_0^0$. The *second order norm* of $\mathbf{S}$, denoted $M = M_0$, is defined as the maximum norm of the following $2n+10$ SOFDs:

$$\begin{aligned}M = max\{&\{\, \|2\mathbf{V}_1 - \mathbf{V}_{2i} - \mathbf{V}_{2((i+1)\%n+1)}\| \mid 1 \le i \le n\} \\ \cup\ &\{\, \|2\mathbf{V}_{2(i\%n+1)} - \mathbf{V}_{2i+1} - \mathbf{V}_{2(i\%n+1)+1}\| \mid 1 \le i \le n\} \\ \cup\ &\{\, \| 2\mathbf{V}_3 - \mathbf{V}_2 - \mathbf{V}_{2n+8} \|,\ \| 2\mathbf{V}_4 - \mathbf{V}_1 - \mathbf{V}_{2n+7} \|, \\ &\| 2\mathbf{V}_5 - \mathbf{V}_6 - \mathbf{V}_{2n+6} \|,\ \| 2\mathbf{V}_5 - \mathbf{V}_4 - \mathbf{V}_{2n+3} \|, \\ &\| 2\mathbf{V}_6 - \mathbf{V}_1 - \mathbf{V}_{2n+4} \|,\ \| 2\mathbf{V}_7 - \mathbf{V}_8 - \mathbf{V}_{2n+5} \|, \\ &\| 2\mathbf{V}_{2n+7} - \mathbf{V}_{2n+6} - \mathbf{V}_{2n+8} \|, \\ &\| 2\mathbf{V}_{2n+6} - \mathbf{V}_{2n+2} - \mathbf{V}_{2n+7} \|, \\ &\| 2\mathbf{V}_{2n+3} - \mathbf{V}_{2n+2} - \mathbf{V}_{2n+4} \|, \\ &\| 2\mathbf{V}_{2n+4} - \mathbf{V}_{2n+3} - \mathbf{V}_{2n+5} \| \,\}\,\}\end{aligned} \tag{3}$$

By performing a subdividion step on Π, one gets $2n+17$ new vertices $\mathbf{V}_i^1$, $i = 1, ..., 2n+17$ (see Figure 3(b)). These control points form four control point sets Π_0^1, Π_1^1, Π_2^1 and Π_3^1, representing control meshes of the subpatches $\mathbf{S}_0^1$, $\mathbf{S}_1^1$, $\mathbf{S}_2^1$ and $\mathbf{S}_3^1$, respectively (see Figure 3(b)) where $\Pi_0^1 = \{\mathbf{V}_i^1 \mid 1 \le i \le 2n+8\}$, and the other three control point sets Π_1^1, Π_2^1 and Π_3^1 are shown in Figure 4. $\mathbf{S}_0^1$ is an extra-ordinary patch but $\mathbf{S}_1^1$, $\mathbf{S}_2^1$ and $\mathbf{S}_3^1$ are regular patches. Therefore, second order norm similar to the one defined in (2) can be defined for $\mathbf{S}_1^1$, $\mathbf{S}_2^1$ and $\mathbf{S}_3^1$, while a second order norm similar to (3) can be defined for the control mesh of $\mathbf{S}_0^1$. We use M_1 to denote the

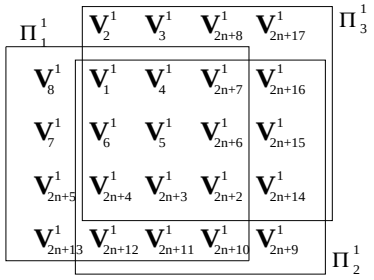

Figure 4: Control vertices of subpatches $\mathbf{S}_1^1$, $\mathbf{S}_2^1$ and $\mathbf{S}_3^1$.

second order norm of $\mathbf{S}_0^1$. This process can be iteratively repeated on $\mathbf{S}_0^1$, $\mathbf{S}_0^2$, $\mathbf{S}_0^3$, ... etc. We have the following lemma for a general $\mathbf{S}_0^k$ and its second order norm M_k [5].

Lemma 2: For any $k \geq 0$, if M_k represents the second order norm of the extra-ordinary sub-patch $\mathbf{S}_0^k$ after k Catmull-Clark subdivision steps, then M_k satisfies the following inequality

$$M_{k+1} \leq \begin{cases} \frac{2}{3}M_k, & n = 3 \\ \frac{18}{25}M_k, & n = 5 \\ (\frac{3}{4} + \frac{8n-46}{4n^2})M_k, & n > 5 \end{cases}.$$

Actually, the lemma works in a more general sense, i.e., if M_k stands for the second order norm of the control mesh $\mathbf{M}_k$, instead of Π_0^k, the lemma still works. The second order norm of $\mathbf{M}_k$ is defined as follows: for regions not involving the extra-ordinary point, use standard SOFDs; for the vicinity of the extra-ordinary point, use SOFDs defined in (3). The proof is essentially the same.

2.5.2 Distance Evaluation

To compute the distance between the extra-ordinary patch $\mathbf{S}(u,v)$ and the center face of its control mesh, $\mathbf{F} = \{\mathbf{V}_1, \mathbf{V}_6, \mathbf{V}_5, \mathbf{V}_4\}$, we need to parameterize the patch $\mathbf{S}(u,v)$ first.

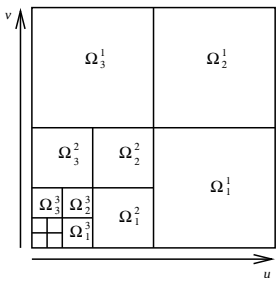

Figure 5: Ω-partition of the unit square.

By iteratively performing Catmull-Clark subdivision on $\mathbf{S}(u,v) = \mathbf{S}_0^0$, $\mathbf{S}_0^1$, $\mathbf{S}_0^2$, ... etc, we get a sequence of regular patches $\{\ \mathbf{S}_b^m\ \}$, $m \geq 1$, $b = 1,2,3$, and a sequence of extra-ordinary patches $\{\ \mathbf{S}_0^m\ \}$, $m \geq 1$. The extra-ordinary patches converge to a limit point which is the value of $\mathbf{S}$ at $(0,0)$ [8]. This limit point and the regular patches $\{\ \mathbf{S}_b^m\ \}$, $m \geq 1$, $b = 1,2,3$, form a partition of $\mathbf{S}$. If we use Ω_b^m to represent the region of the parameter space that corresponds to $\mathbf{S}_b^m$ then $\{\ \Omega_b^m\ \}$, $m \geq 1$, $b = 1,2,3$, form a partition of the unit square $\Omega = [0,1] \times [0,1]$ (see Figure 5) with

$$\begin{aligned} \Omega_1^m &= [\tfrac{1}{2^m}, \tfrac{1}{2^{m-1}}] \times [0, \tfrac{1}{2^m}], \\ \Omega_2^m &= [\tfrac{1}{2^m}, \tfrac{1}{2^{m-1}}] \times [\tfrac{1}{2^m}, \tfrac{1}{2^{m-1}}], \\ \Omega_3^m &= [0, \tfrac{1}{2^m}] \times [\tfrac{1}{2^m}, \tfrac{1}{2^{m-1}}]. \end{aligned} \quad (4)$$

The parametrization of $\mathbf{S}(u,v)$ is done as follows. For any $(u,v) \in \Omega$ but $(u,v) \neq (0,0)$, first find the Ω_b^m that contains (u,v). m and b can be computed as follows.

$$\begin{aligned} m(u,v) &= \min\{\lceil log_{\frac{1}{2}} u \rceil,\ \lceil log_{\frac{1}{2}} v \rceil\} \\ b(u,v) &= \begin{cases} 1, & if\ 2^m u \geq 1\ and\ 2^m v \leq 1 \\ 2, & if\ 2^m u \geq 1\ and\ 2^m v \geq 1 \\ 3, & if\ 2^m u \leq 1\ and\ 2^m v \geq 1 \end{cases} \end{aligned} \quad (5)$$

Then map this Ω_b^m to the unit square with the following mapping

$$(u,v) \rightarrow\ (u_m, v_m)$$

where

$$t_m = (2^m t)\%1 = \begin{cases} 2^m t, & if\ \ 2^m t \leq 1 \\ 2^m t - 1, & if\ \ 2^m t > 1 \end{cases} \quad (6)$$

The value of $\mathbf{S}(u,v)$ is equal to the value of $\mathbf{S}_b^m$ at (u_m, v_m), i.e.,

$$\mathbf{S}(u,v) = \mathbf{S}_b^m(u_m, v_m).$$

Let $\mathbf{L}_b^m(u,v)$ be the bilinear parametrization of the center face of $\mathbf{S}_b^m$'s control mesh. Since $\mathbf{S}_b^m$ is a regular patch, following Lemma 1, we have

$$\|\mathbf{L}_b^m(u,v) - \mathbf{S}_b^m(u,v)\| \leq \frac{1}{3}M_b^m$$

where M_b^m is the second order norm of the contol mesh of $\mathbf{S}_b^m$. The second order norm of $\mathbf{S}_b^m$ is smaller than the second order norm of $\mathbf{M}_m$, M_m. Hence, the above inequality can be written as

$$\|\mathbf{L}_b^m(u,v) - \mathbf{S}_b^m(u,v)\| \leq \frac{1}{3}M_m. \quad (7)$$

If we use $\mathbf{L}(u,v)$ to represent the bilinear parametrization of the center face of $\mathbf{S}(u,v)$'s control mesh $\mathbf{F} = \{\mathbf{V}_1, \mathbf{V}_6, \mathbf{V}_5, \mathbf{V}_4\}$

$$\begin{aligned} \mathbf{L}(u,v) \quad = \quad & (1-v)[(1-u)\mathbf{V}_1 + u\mathbf{V}_6] \\ & +v[(1-u)\mathbf{V}_4 + u\mathbf{V}_5], \quad 0 \leq u,v \leq 1 \end{aligned}$$

then the maximum distance between $\mathbf{S}(u,v)$ and its control mesh can be written as

$$\begin{aligned} &\| \mathbf{L}(u,v) - \mathbf{S}(u,v) \| \\ &\quad \leq \| \mathbf{L}(u,v) - \mathbf{L}_b^m(u_m,v_m)\| + \|\mathbf{L}_b^m(u_m,v_m) - \mathbf{S}(u,v) \| \end{aligned} \tag{8}$$

where $0 \leq u,v \leq 1$ and u_m and v_m are defined in (6). The second term on the right hand side of the inequality can be evaluated using (7). Hence, one only needs to work with the first term on the right hand side of the inequality.

It is easy to see that if $(u,v) \in \Omega_b^m$ then $(u,v) \in \Omega_0^k$ for any $0 \leq k < m$ where

$$\Omega_0^k = [0,\ \frac{1}{2^k}] \times [0,\ \frac{1}{2^k}].$$

Ω_0^k corresponds to the subpatch $\mathbf{S}_0^k$. This means that $(2^k u, 2^k v)$ is within the parameter space of $\mathbf{S}_0^k$ for $0 \leq k < m$, i.e., $(2^k u, 2^k v) = (u_k, v_k)$ where u_k and v_k are defined in (6). Consequently, we can consider $\mathbf{L}_0^k(u_k,v_k)$ for $0 \leq k < m$ where $\mathbf{L}_0^k$ is the bilinear parametrization of the center face of the control mesh of $\mathbf{S}_0^k$ (with the understanding that $\mathbf{L}_0^0 = \mathbf{L}$ and $(u_0,v_0) = (u,v)$). Hence, the first term on the right hand side of (8) can be written as

$$\begin{aligned} &\|\mathbf{L}(u,v) - \mathbf{L}_b^m(u_m,v_m)\| \\ &\quad \leq \textstyle\sum_{k=0}^{m-2} \|\mathbf{L}_0^k(u_k,v_k) - \mathbf{L}_0^{k+1}(u_{k+1},v_{k+1})\| \\ &\qquad + \|\mathbf{L}_0^{m-1}(u_{m-1},v_{m-1}) - \mathbf{L}_b^m(u_m,v_m)\|. \end{aligned} \tag{9}$$

The following two lemmas are needed in the evaluation of the right side of the above inequality.

Lemma 3: If $(u,v) \in \Omega_b^m$ where b and m are defined in (5) then for any $0 \leq k < m-1$ we have

$$\| \mathbf{L}_0^k(u_k,v_k) - \mathbf{L}_0^{k+1}(u_{k+1},v_{k+1}) \| \leq \frac{1}{\min\{\ n, 8\ \}} M_k$$

where M_k is the second order norm of $\mathbf{M}_k$ and $\mathbf{L}_0^0 = \mathbf{L}$.

Lemma 4: If $(u,v) \in \Omega_b^m$ where b and m are defined in (5) then we have

$$\begin{aligned} &\| \mathbf{L}_0^{m-1}(u_{m-1},v_{m-1}) - \mathbf{L}_b^m(u_m,v_m) \| \\ &\quad \leq \begin{cases} \frac{1}{4} M_{m-1}, & if \quad b = 2 \\ \frac{1}{8} M_{m-1}, & if \quad b = 1 \ or \ 3 \end{cases} \end{aligned}$$

where M_{m-1} is the second order norm of $\mathbf{M}_{m-1}$.

By applying Lemmas 3 and 4 on (9) and then using (7) on (8), we have the following lemma on the distance between an extra-ordinary CCSS patch $\mathbf{S}(u,v)$ and its control mesh $\mathbf{L}(u,v)$ [5].

Lemma 5: The maximum of $\| \mathbf{L}(u,v) - \mathbf{S}(u,v) \|$ satisfies the following inequality

$$\| \mathbf{L}(u,v) - \mathbf{S}(u,v) \| \leq \begin{cases} M_0, & n = 3 \\ \frac{5}{7} M_0, & n = 5 \\ \frac{4n}{n^2 - 8n + 46} M_0, & 5 < n \leq 8 \\ \frac{n^2}{4(n^2 - 8n + 46)} M_0, & n > 8 \end{cases} \tag{10}$$

where $M = M_0$ is the second order norm of the extra-ordinary patch $\mathbf{S}(u,v)$.

2.5.3 Subdivision Depth Computation

Lemma 5 can be used to estimate the distance between a level-k control mesh and the surface patch for any $k > 0$. This is because the distance between a level-k control mesh and the surface patch is dominated by the distance between the level-k extra-ordinary subpatch and the corresponding control mesh which, accoriding to Lemma 5, is

$$\| \mathbf{L}_k(u,v) - \mathbf{S}(u,v) \| \leq \begin{cases} M_k, & n = 3 \\ \frac{18}{25} M_k, & 5 \leq n \leq 8 \\ \frac{n^2}{4(n^2 - 8n + 46)} M_k, & n > 8 \end{cases}$$

where M_k is the second order norm of $\mathbf{S}(u,v)$'s level-k control mesh $\mathbf{M}_k$. The previous subdivision depth computation technique for extra-ordinary surface patches is obtained by combining the above result with Lemma 2 [5].

Theorem 6: Given an extra-ordinary surface patch $\mathbf{S}(u,v)$ and an error tolerance ϵ, if k levels of subdivisions are iteratively performed on the control mesh of $\mathbf{S}(u,v)$, where

$$k = \left\lceil log_w \frac{M}{z\epsilon} \right\rceil$$

with M being the second order norm of $\mathbf{S}(u,v)$ defined in (3),

$$w = \begin{cases} \frac{3}{2}, & n = 3 \\ \frac{25}{18}, & n = 5 \\ \frac{4n^2}{3n^2 + 8n - 46}, & n > 5 \end{cases}$$

and

$$z = \begin{cases} 1, & n = 3 \\ \frac{25}{18}, & 5 \leq n \leq 8 \\ \frac{2(n^2 - 8n + 46)}{n^2}, & n > 8 \end{cases}$$

then the distance between $\mathbf{S}(u,v)$ and the level-k control mesh is smaller than ϵ.

3 New Subdivision Depth Computation Technique for Extra-Ordinary Patches

The SOFDs involved in the second order norm of an extra-ordinary CCSS patch (see eq. (3)) can be classified into two groups: *group I* and *group II*. Group I contains those SOFDs that involve vertices in the vicinity of the extra-ordinary vertex (see Figure 6(a)). These are the first $2n$ SOFDs in (3). Group II contains the remaining SOFDs, i.e., SOFDs that involve vertices in the vicinity of the other three vertices of $\mathbf{S}$ (see Figure 6(b)). These are the last 10 SOFDs in (3). It is easy to see that the convergence rate of the SOFDs in group II is the same as the regular case, i.e., 1/4 [4]. Therefore, to study properties of the second order norm M, it is sufficient to study norms of the SOFDs in group I. The maximum of these norms will be called the *second order norm* of group I. We will use $M = M_0$ to represent group I's second order norm as well because norms of group I's SOFDs dominate norms of group II's SOFDs. For convenience of reference, in the subsequent discussion we shall simply use the term "second order norm of an extra-ordinary CCSS patch" to refer to the "second order norm of group I of an extra-ordinary CCSS patch".

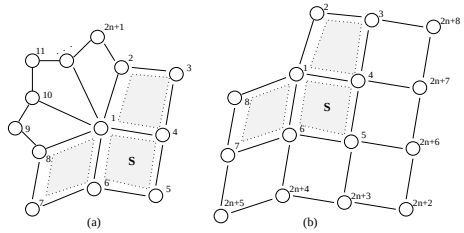

Figure 6: (a) Vicinity of the extra-ordinary point. (b) Vicinity of the other three vertices of $\mathbf{S}$.

3.1 Matrix based Rate of Convergence

The second order norm of $\mathbf{S} = \mathbf{S}_0^0$ can be put in matrix form as follows:

$$M = \|\mathrm{A}\mathbf{P}\|_\infty$$

where A is a $2n * (2n+1)$ matrix

$$\mathrm{A} = \begin{bmatrix} 2 & -1 & 0 & 0 & 0 & -1 & 0 & 0 & \cdots & 0 & 0 \\ 2 & 0 & 0 & -1 & 0 & 0 & 0 & -1 & \cdots & 0 & 0 \\ 2 & 0 & 0 & 0 & 0 & -1 & 0 & 0 & \cdots & 0 & 0 \\ & & & & \vdots & & & & & & \\ 2 & 0 & 0 & -1 & 0 & 0 & 0 & 0 & \cdots & -1 & 0 \\ 0 & 2 & -1 & 0 & 0 & 0 & 0 & 0 & \cdots & 0 & -1 \\ 0 & 0 & -1 & 2 & -1 & 0 & 0 & 0 & \cdots & 0 & 0 \\ & & & & \vdots & & & & & & \\ 0 & 0 & 0 & 0 & 0 & 0 & 0 & 0 & \cdots & 2 & -1 \end{bmatrix}$$

and $\mathbf{P}$ is a control point vector

$$\mathbf{P} = [\mathbf{V}_1,\ \mathbf{V}_2,\ \mathbf{V}_3, \ldots,\ \mathbf{V}_{2n+1}]^T.$$

A is called the *second order norm matrix* for extra-ordinary CCSS patches. If i levels of Catmull-Clark subdivision are performed on the control mesh of $\mathbf{S} = \mathbf{S}_0^0$ then, following the notation of Section 2, we have an extra-ordinary subpatch $\mathbf{S}_0^i$ whose second order norm can be expressed as:

$$M_i = \left\|\mathrm{A}\Lambda^i\mathbf{P}\right\|_\infty$$

where Λ is a subdivision matrix of dimension $(2n+1) * (2n+1)$. The function of Λ is to perform a subdivision step on the $2n+1$ control vertices around (and including) the extra-ordinary point (see Figure 6(a)). For example, when $n = 3$, Λ is of the following form:

$$\Lambda = \begin{bmatrix} 5/12 & 1/6 & 1/36 & 1/6 & 1/36 & 1/6 & 1/36 \\ 3/8 & 3/8 & 1/16 & 1/16 & 0 & 1/16 & 1/16 \\ 1/4 & 1/4 & 1/4 & 1/4 & 0 & 0 & 0 \\ 3/8 & 1/16 & 1/16 & 3/8 & 1/16 & 1/16 & 0 \\ 1/4 & 0 & 0 & 1/4 & 1/4 & 1/4 & 0 \\ 3/8 & 1/16 & 0 & 1/16 & 1/16 & 3/8 & 1/16 \\ 1/4 & 1/4 & 0 & 0 & 0 & 1/4 & 1/4 \end{bmatrix}.$$

We are interested in knowing the relationship between $\|\mathrm{A}\mathbf{P}\|_\infty$ and $\left\|\mathrm{A}\Lambda^i\mathbf{P}\right\|_\infty$. We need the following important result for $\mathrm{A}\Lambda^i$. The proof of this result is shown in the Appendix.

Lemma 7: $\mathrm{A}\Lambda^i = \mathrm{A}\Lambda^i\mathrm{A}^+\mathrm{A}$, where A^+ is the *pseudo-inverse matrix* of A.

With this lemma, we have

$$\frac{\left\|\mathrm{A}\Lambda^i\mathbf{P}\right\|_\infty}{\|\mathrm{A}\mathbf{P}\|_\infty} = \frac{\left\|\mathrm{A}\Lambda^i\mathrm{A}^+\mathrm{A}\mathbf{P}\right\|_\infty}{\|\mathrm{A}\mathbf{P}\|_\infty} \leq \frac{\left\|\mathrm{A}\Lambda^i\mathrm{A}^+\right\|_\infty \|\mathrm{A}\mathbf{P}\|_\infty}{\|\mathrm{A}\mathbf{P}\|_\infty}$$
$$= \left\|\mathrm{A}\Lambda^i\mathrm{A}^+\right\|_\infty$$

Use r_i to represent $\left\|\mathrm{A}\Lambda^i\mathrm{A}^+\right\|_\infty$. Then we have the following recurrence formula for r_i

$$\begin{aligned} r_i &\equiv \left\|\mathrm{A}\Lambda^i\mathrm{A}^+\right\|_\infty = \left\|\mathrm{A}\Lambda^{i-1}\mathrm{A}^+\mathrm{A}\Lambda\mathrm{A}^+\right\|_\infty \\ &\leq \left\|\mathrm{A}\Lambda^{i-1}\mathrm{A}^+\right\|_\infty \ \|\mathrm{A}\Lambda\mathrm{A}^+\|_\infty \qquad (11) \\ &= r_{i-1}\ r_1 \end{aligned}$$

where $r_0 = 1$. Hence, we have the following lemma on the convergence rate of second order norm of an extra-ordinary CCSS patch.

Lemma 8: The second order norm of an extra-ordinary CCSS patch satisfies the following inquality:

$$M_i \leq r_i\ M_0 \qquad (12)$$

where $r_i = \left\|\mathrm{A}\Lambda^i\mathrm{A}^+\right\|_\infty$ and r_i satisfies the recurrence formula (11).

The recurrence formula (11) shows that r_i in (12) can be replaced with r_1^i. However, experiment data show that,

while the convergence rate changes by a constant ratio in most of the cases, there is a significant difference between r_2 and r_1. The value of r_2 is smaller than r_1^2 by a significant gap. Hence, if we use r_1^i for r_i in (12), we would end up with a bigger subdivision depth for a given error tolerance. A better choice is to use r_2 to bound r_i, as follows.

$$r_i \leq \begin{cases} r_2^j, & \text{i} = 2j \\ r_1 r_2^j, & \text{i} = 2j+1 \end{cases} \tag{13}$$

3.2 Distance Evaluation

Following (8) and (9), the distance between the extra-ordinary CCSS patch $\mathbf{S}(u,v)$ and the center face of its control mesh $\mathbf{L}(u,v)$ can be expressed as

$$\begin{aligned} &\|\mathbf{L}(u,v) - \mathbf{S}(u,v)\| \\ &\leq \textstyle\sum_{k=0}^{m-2} \|\mathbf{L}_0^k(u_k,v_k) - \mathbf{L}_0^{k+1}(u_{k+1},v_{k+1})\| \\ &\quad + \|\mathbf{L}_0^{m-1}(u_{m-1},v_{m-1}) - \mathbf{L}_b^m(u_m,v_m)\| \\ &\quad + \|\mathbf{L}_b^m(u_m,v_m) - \mathbf{S}_b^m(u_m,v_m)\| \end{aligned} \tag{14}$$

where m and b are defined in (5) and (u_i, v_i) are defined in (6). By applying Lemma 3, Lemma 4 and (7) on the first, second and third terms of the right hand side of the above inequality, respectively, we get

$$\begin{aligned} \|\mathbf{L}(u,v) - \mathbf{S}(u,v)\| &\leq c\textstyle\sum_{k=0}^{m-2} M_k + \frac{1}{4}M_{m-1} + \frac{1}{3}M_m \\ &\leq M_0(c\textstyle\sum_{k=0}^{m-2} r_k + \frac{1}{4}r_{m-1} + \frac{1}{3}r_m) \end{aligned}$$

where $c = 1/\min\{n, 8\}$. The last part of the above inequality follows from Lemma 8. Consequently, through a simple algebra, we have

$$\|\mathbf{L}(u,v) - \mathbf{S}(u,v)\| \leq \begin{cases} M_0[c(\frac{1-r_2^j}{1-r_2} + \frac{1-r_2^{j-1}}{1-r_2} r_1) \\ \quad + \frac{r_1 r_2^{j-1}}{4} + \frac{r_2^j}{3}], & \text{if } m = 2j \\ M_0[c(\frac{1-r_2^j}{1-r_2} + \frac{1-r_2^j}{1-r_2} r_1) \\ \quad + \frac{r_2^j}{4} + \frac{r_1 r_2^j}{3}], & \text{if } m = 2j+1 \end{cases}$$

It can be easily proved that the maximum occurs at $m = \infty$. Hence, we have the following lemma.

Lemma 9: The maximum of $\|\mathbf{L}(u,v) - \mathbf{S}(u,v)\|$ satisfies the following inequality

$$\|\mathbf{L}(u,v) - \mathbf{S}(u,v)\| \leq \frac{M_0}{\min\{n,8\}} \frac{1+r_1}{1-r_2}$$

where $r_i = \|\mathrm{A}\Lambda^i\mathrm{A}^+\|_\infty$ and $M = M_0$ is the second order norm of the extra-ordinary patch $\mathbf{S}(u,v)$.

3.3 Subdivision Depth Computation

Lemma 9 can also be used to evaluate the distance between a level-i control mesh and the extra-ordinary patch $\mathbf{S}(u,v)$ for any $i > 0$. This is because the distance between a level-i control mesh and the surface patch $\mathbf{S}(u,v)$ is dominated by the distance between the level-i extra-ordinary subpatch and the corresponding control mesh which, accoriding to Lemma 9, is

$$\|\mathbf{L}_i(u,v) - \mathbf{S}(u,v)\| \leq \frac{M_i}{\min\{n,8\}} \frac{1+r_1}{1-r_2}$$

where M_i is the second order norm of $\mathbf{S}(u,v)$'s level-i control mesh, $\mathbf{M}_i$. Hence, if the right side of the above inequality is smaller than a given error tolerance ϵ, then the distance between $\mathbf{S}(u,v)$ and the level-i control mesh is smaller than ϵ. Consequently, we have the following subdivision depth computation theorem for extra-ordinary CCSS patches.

Theorem 10: Given an extra-ordinary surface patch $\mathbf{S}(u,v)$ and an error tolerance ϵ, if

$$i \equiv \min\{2l,\ 2k+1\}$$

levels of subdivision are iteratively performed on the control mesh of $\mathbf{S}(u,v)$, where

$$l = \lceil \log_{\frac{1}{r_2}} (\tfrac{1}{\min\{n,8\}} \tfrac{1+r_1}{1-r_2} \tfrac{M_0}{\epsilon}) \rceil ,$$

$$k = \lceil \log_{\frac{1}{r_2}} (\tfrac{r_1}{\min\{n,8\}} \tfrac{1+r_1}{1-r_2} \tfrac{M_0}{\epsilon}) \rceil$$

with $r_i = \|\mathrm{A}\Lambda^i\mathrm{A}^+\|_\infty$ and M_0 being the second order norm of $\mathbf{S}(u,v)$, then the distance between $\mathbf{S}(u,v)$ and the level-i control mesh is smaller than ϵ.

4 Examples

The new subdivision depth technique has been inplemented in *C++* on the Windows platform to compare its performance with the previous approach. *MatLab* is used for both numerical and symbolic computation of r_i in the implementation. Table 1 shows the comparison results of the previous technique, Theorem 6, with the new technique, Theorem 10. Two error tolerances 0.01 and 0.001 are considered and the second order norm M_0 is assumed to be 2. For each error tolerance, we consider five different valences: 3, 5, 6, 7 and 8 for the extra-ordinary vertex. As can be seen from the table, the new technique has a 30% improvement over the previous technique in most of the cases. Hence, the new technique indeed improves the previous technique significantly.

To show that the rates of convergence are indeed difference between r_1 and r_2, their values from several typical extra-ordinary CCSS patches are included in Table 2. Note that when we compare r_1 and r_2, the value of r_1 should be squared first.

Table 1. Comparison between the old technique and the new technique

	$\epsilon = 0.01$		$\epsilon = 0.001$	
N	Old Technique	New Technique	Old Technique	New Technique
3	14	9	19	12
5	16	11	23	16
6	19	16	27	22
7	23	14	33	22
8	37	27	49	33

Table 2. Values of r_1 and r_2 for some extra-ordinary patches.

N	r_1	r_2
3	0.6667	0.2917
5	0.7200	0.4016
6	0.8889	0.5098
7	0.8010	0.5121
8	1.0078	0.5691

5 Conclusions

A new subdivision depth computation technique for extra-ordinary CCSS patches is presented. Like the previous technique, the subdivision depth is computed based on norms of the second order forward differences of the control points. However, the computation process is performed on matrix representation of the second order norm, which gives us a better bound of the convergence rate and, consequently, a tighter subdivision depth for a given error tolerance. Test results show that the new technique improves the previous technique by about 30% in most of the cases. This is a significant result because of the exponential nature of the subdivision process. We are not sure if the new technique can be further improved though.

6 Appendix A: Proof of Lemma 7

It can be shown that when n is odd, i.e, when $n = 2k+1$ for some positivi integer k, $\mathrm{A}^+\mathrm{A}$ is a $(2n+1) \times (2n+1)$ circulant matrix of the following form (see complete version of the paper [3] for proof)

$$\mathrm{A}^+\mathrm{A} = \mathrm{H} \equiv \frac{1}{2n+1} \begin{bmatrix} 2n & -1 & \cdots & -1 & -1 \\ -1 & 2n & \cdots & -1 & -1 \\ & & \vdots & & \\ -1 & -1 & \cdots & 2n & -1 \\ -1 & -1 & \cdots & -1 & 2n \end{bmatrix}. \quad (15)$$

When n is an even number of the form $n = 4k+2$ where k is a positive integer, $\mathrm{A}^+\mathrm{A}$ has the form [3]

$$\mathrm{A}^+\mathrm{A} = \mathrm{H} + \mathrm{E} \quad (16)$$

where H is defined in (15) and

$$\mathrm{E} = \frac{1}{n} \begin{bmatrix} 0 & 0 & 0 & 0 & 0 & 0 & \cdots & 0 \\ 0 & 0 & 0 & 0 & 0 & 0 & \cdots & 0 \\ 0 & 0 & -1 & 0 & 1 & 0 & \cdots & 1 \\ 0 & 0 & 0 & 0 & 0 & 0 & \cdots & 0 \\ 0 & 0 & 1 & 0 & -1 & 0 & \cdots & -1 \\ 0 & 0 & 0 & 0 & 0 & 0 & \cdots & 0 \\ & & \vdots & & \vdots & & & \\ 0 & 0 & -1 & 0 & 1 & 0 & \cdots & 1 \\ 0 & 0 & 0 & 0 & 0 & 0 & \cdots & 0 \\ 0 & 0 & 1 & 0 & -1 & 0 & \cdots & -1 \end{bmatrix}. \quad (17)$$

When $n = 4k$, $\mathrm{A}^+\mathrm{A}$ has the form [3]

$$\mathrm{A}^+\mathrm{A} = \mathrm{H} + \mathrm{E} + \mathrm{W} + \mathrm{Z} \quad (18)$$

where H is defined in (15), E is defined in (17),

$$\mathrm{W} = \frac{2}{3n} \begin{bmatrix} 0 & 0 & 0 & 0 & 0 & \cdots & 0 \\ 0 & -1 & 0 & 0 & 0 & \cdots & 0 \\ 0 & -1 & 0 & -1 & 0 & \cdots & 0 \\ 0 & 0 & 0 & -1 & 0 & \cdots & 0 \\ 0 & 1 & 0 & -1 & 0 & \cdots & 0 \\ 0 & 1 & 0 & 0 & 0 & \cdots & 0 \\ 0 & 1 & 0 & 1 & 0 & \cdots & 0 \\ 0 & 0 & 0 & 1 & 0 & \cdots & 0 \\ 0 & -1 & 0 & 1 & 0 & \cdots & 0 \\ & \vdots & & \vdots & & & \\ 0 & 0 & 0 & 1 & 0 & \cdots & 0 \\ 0 & -1 & 0 & 1 & 0 & \cdots & 0 \end{bmatrix},$$

and

$$\mathrm{Z} = \frac{2}{3n} \begin{bmatrix} 0 & 0 & 0 & 0 & 0 & 0 & \cdots & 0 \\ 0 & 0 & -1 & 0 & 1 & 0 & \cdots & 1 \\ 0 & 0 & -2 & 0 & 0 & 0 & \cdots & 0 \\ 0 & 0 & -1 & 0 & -1 & 0 & \cdots & -1 \\ 0 & 0 & 0 & 0 & -2 & 0 & \cdots & -2 \\ 0 & 0 & 1 & 0 & -1 & 0 & \cdots & -1 \\ 0 & 0 & 2 & 0 & 0 & 0 & \cdots & 0 \\ 0 & 0 & 1 & 0 & 1 & 0 & \cdots & 1 \\ 0 & 0 & 0 & 0 & 2 & 0 & \cdots & 2 \\ & & \vdots & & \vdots & & & \\ 0 & 0 & 1 & 0 & 1 & 0 & \cdots & 1 \\ 0 & 0 & 0 & 0 & 2 & 0 & \cdots & 2 \end{bmatrix}.$$

We prove the lemma for the case $n = 2k+1$ first. Let F be a $(2n+1) * (2n+1)$ Fourier transform matrix

$$\mathrm{F} = \frac{1}{\sqrt{2n+1}} \begin{bmatrix} 1 & 1 & 1 & \cdots & 1 & 1 \\ 1 & \omega & \omega^2 & \cdots & \omega^{2n-1} & \omega^{2n} \\ 1 & \omega^2 & \omega^4 & \cdots & \omega^{4n-2} & \omega^{4n} \\ \vdots & & & \vdots & & \vdots \\ 1 & \omega^{2n} & \omega^{4n} & \cdots & \omega^{4n^2-2n} & \omega^{4n^2} \end{bmatrix}$$

where $\omega = e^{2\pi i/(2n+1)}$. It is easy to see from eq.(15) that

$$\mathrm{F}^*\mathrm{HF} = \mathrm{I} - \begin{bmatrix} 1 & 0 & \cdots & 0 \\ 0 & 0 & \cdots & 0 \\ \vdots & \vdots & & \vdots \\ 0 & 0 & \cdots & 0 \end{bmatrix}$$

where I is a $(2n+1) * (2n+1)$ identity matrix. Hence, when $n = 2k+1$ we have

$$\begin{aligned} \mathrm{A}\Lambda^i\mathrm{A}^+\mathrm{A} &= \mathrm{A}\Lambda^i\mathrm{H} = \mathrm{A}\Lambda^i\mathrm{FF}^*\mathrm{HFF}^* \\ &= \mathrm{A}\Lambda^i\mathrm{F}(\mathrm{I} - \begin{bmatrix} 1 & 0 & \cdots & 0 \\ 0 & 0 & \cdots & 0 \\ \vdots & & & \vdots \\ 0 & 0 & \cdots & 0 \end{bmatrix})\mathrm{F}^* \\ &= \mathrm{A}\Lambda^i - \mathrm{A}\Lambda^i\mathrm{F}\begin{bmatrix} 1 & 0 & \cdots & 0 \\ 0 & 0 & \cdots & 0 \\ \vdots & & & \vdots \\ 0 & 0 & \cdots & 0 \end{bmatrix}\mathrm{F}^* \\ &= \mathrm{A}\Lambda^i - \mathrm{A}\Lambda^i\begin{bmatrix} 1 & 1 & \cdots & 1 \\ 1 & 1 & \cdots & 1 \\ \vdots & & & \vdots \\ 1 & 1 & \cdots & 1 \end{bmatrix}. \end{aligned}$$

Note that

$$\mathrm{A}\Lambda^i\begin{bmatrix} 1 & 1 & \cdots & 1 \\ 1 & 1 & \cdots & 1 \\ \vdots & & & \vdots \\ 1 & 1 & \cdots & 1 \end{bmatrix} = 0$$

because the row sum of A is 0 and row sum of Λ is 1. Hence, we have $\mathrm{A}\Lambda^i = \mathrm{A}\Lambda^i\mathrm{A}^+\mathrm{A}$ when $n = 2k+1$.

We next prove the lemma for $n = 4k+2$. Note that in this case $\Lambda\mathrm{E} = \frac{1}{4}\mathrm{E}$ and $\mathrm{AE} = 0$. With these results we have

$$\mathrm{A}\Lambda^i\mathrm{E} = \frac{1}{4^i}\mathrm{AE} = 0.$$

Hence, $\mathrm{A}\Lambda^i\mathrm{A}^+\mathrm{A} = \mathrm{A}\Lambda^i(\mathrm{H}+\mathrm{E}) = \mathrm{A}\Lambda^i$.

Finally, we prove the lemma for $n = 4k$. Similar to the previous case, we can prove that $\Lambda\mathrm{W} = \frac{1}{2}\mathrm{W}$, $\mathrm{AW} = 0$ and $\Lambda\mathrm{Z} = \frac{1}{2}\mathrm{Z}_1$, $\mathrm{AZ} = 0$. Therefore, we have $\mathrm{A}\Lambda^i\mathrm{W} = \frac{1}{2^i}\mathrm{AW} = 0$ and $\mathrm{A}\Lambda^i\mathrm{Z} = \frac{1}{2^i}\mathrm{AZ} = 0$. Hence, $\mathrm{A}\Lambda^i\mathrm{A}^+\mathrm{A} = \mathrm{A}\Lambda^i(\mathrm{H}+\mathrm{EW}+\mathrm{Z}) = \mathrm{A}\Lambda^i$.

References

[1] Biermann H, Kristjansson D, Zorin D, Approximate Boolean Operations on Free-Form Solids, *Proceedings of SIGGRAPH 2001*, 185-194.

[2] Catmull E, Clark J, Recursively Generated B-spline Surfaces on Arbitrary Topological Meshes, *Computer-Aided Design 10*, 6, 350-355, 1978.

[3] Chen G, Cheng F, Matrix based Subdivision Depth Computation for Extra-Ordinary Catmull-Clark Subdivision Surface Patches, http://www.cs.uky.edu/∼cheng/PUBL/sub_depth_3.pdf

[4] Cheng F, Yong J, Subdivision Depth Computation for Catmull-Clark Subdivision Surfaces, *Computer Aided Design & Applications 3*, 1-4, 2006.

[5] Cheng F, Chen G, Yong J, Subdivision Depth Computation for Extra-Ordinary Catmull-Clark Subdivision Surface Patches, to appear in *Lecture Notes in Computer Science*, Springer, 2006.

[6] DeRose T, Kass M, Truong T, Subdivision Surfaces in Character Animation, *Proceedings of SIGGRAPH 1998*, 85-94.

[7] Doo D, Sabin M, Behavior of Recursive Division Surfaces near Extraordinary Points, *Computer-Aided Design 10*, 6, 356-360, 1978.

[8] Halstead M, Kass M, DeRose T, Efficient, Fair Interpolation Using Catmull-Clark Surfaces, *Proceedings of SIGGRAPH 1993*, 35-44.

[9] Lai S, Cheng F, Parametrization of Catmull-Clark Subdivision Surfaces and its Applications, *Computer Aided Design & Applications 3*, 1-4, 2006.

[10] Litke N, Levin A, Schröder P, Trimming for Subdivision Surfaces, *Computer Aided Geometric Design 18*, 5, 463-481, 2001.

[11] Lutterkort D, Peters J, Tight linear envelopes for splines, *Numerische Mathematik 89*, 4, 735-748, 2001.

[12] Peters J, Patching Catmull-Clark Meshes, *Proceedings of SIGGRAPH 2000*, 255-258.

[13] Sederberg T W, Zheng J, Sewell D, Sabin M, Non-Uniform Recursive Subdivision Surfaces, *Proceedings of SIGGRAPH 1998*, 387-394.

[14] Stam J, Exact Evaluation of Catmull-Clark Subdivision Surfaces at Arbitrary Parameter Values, *Proceedings of SIGGRAPH 1998*, 395-404.

[15] Stam J, Evaluation of Loop Subdivision Surfaces, *SIGGRAPH'99 Course Notes*, 1999.

[16] Wang H, Qin K, 2004. Estimating Subidivision Depth of Catmull-Clark Surfaces. *J. Comput. Sci. & Technol. 19*, 5, 657-664.

[17] Wu X, Peters J, An Accurate Error Measure for Adaptive Subdivision Surfaces, *Proc. Shape Modeling International 2005*, 1-6.

[18] Zorin, D., Schröder, P., and Sweldens, W. Interactive Multiresolution Mesh Editing. *Proceedings of SIGGRAPH 1997*, 259-268.

[19] Zorin D, Kristjansson D, Evaluation of Piecewise Smooth Subdivision Surfaces, *The Visual Computer*, 18(5/6):299-315, 2002.